The system K_2O–Al_2O_3–SiO_2. Part 1. Phases on the $KAlSiO_4$–$KAlO_2$ join

L. P. Cook, R. S. Roth, H. S. Parker and T. Negas

National Bureau of Standards, Washington, D.C. 20234

Abstract

High-temperature experiments have yielded information about the part of the tectosilicate join between $KAlSiO_4$ and $KAlO_2$. Orthorhombic $KAlSiO_4$ synthesized at 950°C [a = 9.057(2), b = 15.642(2), c = 8.582(2)A], space group $P2_12_12$ transforms upon heating above 1450–1485°C to another orthorhombic phase having a larger unit cell [a = 18.110(3), b = 15.600(3), c = 8.560(2)A]. The space group of the latter is shown from single-crystal precession photographs to be one of three possibilities: $P2_1am$, $Pma2$, or $Pmam$.

A body-centered tetragonal phase, $K_{1+x}Al_{1+x}Si_{1-x}O_4$ ($x \approx 0.1$), with unit-cell dimensions a = 8.943(1), c = 5.221(1)A is stable at the expense of orthorhombic $KAlSiO_4$ and silica-saturated $KAlO_2$ solid solution in the range 1400–1600°C. Five space groups within Laue group $4/mmm$ are possibilities.

The compound previously reported to be $K_2Al_2SiO_6$ is most likely a member of the f.c.c. solid solution $K_{1-x}Al_{1-x}Si_xO_2$. The SiO_2-rich end-member of this solid solution has a composition with $x \approx 0.25$ at 1600°C, and apparently belongs to Laue group $m3m$.

Introduction

Research is being conducted in our laboratories to determine the effect of K_2O on the behavior of refractory oxide materials and the properties of silicate melts in open-cycle, coal-fired magnetohydrodynamic (MHD) power generators. One of the areas most important to this research is the silica-poor part of the system K_2O–Al_2O_3–SiO_2. Hexagonal and orthorhombic $KAlSiO_4$ have been shown to be important phases in MHD systems (Karr *et al.*, 1974; Hosler *et al.*, 1976). The natural occurrence of hexagonal $KAlSiO_4$ in igneous rocks, either as kalsilite or kaliophilite, is well-known. In this paper we present experimental results for the join $KAlSiO_4$–$KAlO_2$, including the crystallographic properties of two new phases having compositions corresponding to or in close proximity to $KAlSiO_4$. A more detailed study of the phase relations along this join is in progress.

Previous studies

$KAlSiO_4$

The polymorphism of $KAlSiO_4$ was demonstrated in the early work by Bowen (1917). Subsequently, $KAlSiO_4$ polymorphs have been the subject of a number of investigations because of their complicated structure. Rigby and Richardson (1947) possibly were the first to report an X-ray powder pattern (unindexed) for an orthorhombic form of $KAlSiO_4$. Other studies completed prior to 1950 are summarized and discussed by Kunze (1954). Smith and Tuttle (1957) reviewed the crystallographic data and presented new data describing five possible polymorphs of $KAlSiO_4$, four of which were indicated as being hexagonal. Sahama and Smith (1957) reported a fifth hexagonal polymorph. Perrota and Smith (1965) reported a structure determination of hexagonal kalsilite.

"$K_2Al_2SiO_6$"

Weyberg (1908) reported the synthesis from kaolin and potassium chromate of octahedra which he identified as $K_2Al_2SiO_6$. Bowen (1917, p. 118) reported the synthesis of similar octahedra (n = 1.540) by fusing silica, alumina, and KF over a bunsen burner. However, subsequent chemical analysis, which led to the formulation $K_2Al_2SiO_6$, was performed on a two-phase mixture. Schairer and Bowen (1955, p. 735) reported unsuccessful attempts to synthesize $K_2Al_2SiO_6$ by reacting K_2SiO_3 and Al_2O_3 at 1400 to 1700°C. Yamaguchi (1970) listed a unit cell of 7.650(5)A for a cubic compound described as $K_2Al_2SiO_6$, and synthesized by exposing mullite to K_2CO_3 vapor at 1100–1200°C. Evidence was pre-

sented for a complete series of solid solutions be-
tween $K_2Al_2SiO_6$ and $KAlO_2$. Li *et al.* (1971) reported
a maximum solubility of SiO_2 in $KAlO_2$ of 20 mole
percent at 900°C.

$KAlO_2$

Brownmiller (1935) gave an unindexed powder
pattern for cubic $KAlO_2$ ($n = 1.603$) synthesized at
1650°C. Barth (1935) drew attention to the similarity
between cubic $KAlO_2$ and the cristobalite structure.
More recent work (Otsubo *et al.*, 1962; Arakelyan,
1960) has shown the cubic modification of the pure
substance to be unstable at room temperature, with
an unquenchable transformation to a lower-symme-
try form at 522°–535°C.

Methods

Starting materials

$KAlO_2$, used to prepare compositions along the
$KAlO_2$–SiO_2 join, was synthesized from research-
grade anhydrous K_2CO_3 (0.05 wt % Na) and alumina
having 0.3 μm average particle size. The latter yields a
well-defined X-ray powder diffraction pattern for α-
Al_2O_3, and spectrochemical analysis showed less than
0.01 weight percent Na or Fe. Both K_2CO_3 and Al_2O_3
were stored at 160°C until use. K_2CO_3 stored in this
way, cooled under vacuum, weighed in a drybox,
heated at 400°C for 16 hours and reweighed gave a
0.01 weight percent loss. Alumina handled similarly,
but heated at 1100°C for 8 hours, showed 0.33 weight
percent loss. Alumina and K_2CO_3 were weighed in
the proper proportions to yield $KAlO_2$ in a nitrogen
atmosphere containing less than 20 ppm H_2O.
Twenty-gram batches of this mixture were homoge-
nized and heated at 800° (3–24 hr), 900° (1–15 hr),
and 1000°C (0.5–1.0 hr). This process was repeated
three times, and the reaction product was cooled in a
dessicator and unloaded in a drybox. A sample of the
product was mixed with petroleum jelly to avoid
rapid hydration during X-ray analysis, which proved
it to be the well-crystallized, low-temperature form of
$KAlO_2$ (single phase). K_2O loss from $KAlO_2$ in cov-
ered crucibles was negligible at these temperatures, as
would be expected from the available vaporization
data (Plante *et al.*, 1975).

Silica was processed from optical-quality colorless
Brazilian quartz, free from inclusions. This was pul-
verized in a steel mortar and pestle to pass a 200-
mesh sieve. Steel particles were removed with a mag-
net, and the material was boiled twice in 6N HCl for
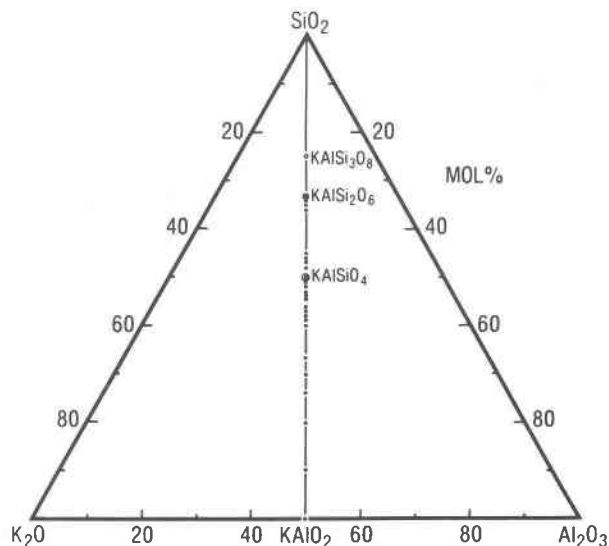several hours, then boiled in distilled water with re-

Fig. 1. Ternary plot showing compositions investigated. Com-
pounds on the tectosilicate join are shown for reference.

peated rinsing and elutriation. For most experiments,
quartz was ground again in an agate mortar and
pestle, and was then stored at 160°C prior to use.
This material showed no detectable weight loss after
heating for 10 hours at 1100°C, and semi-quan-
titative spectrochemical analysis showed less than
0.01 weight percent Fe and less than 0.02 weight
percent Al. For the flux syntheses a commercial high-
purity crystalline silica of 1.5 μm average particle size
was used. Spectrochemical analysis of this material
gave 0.1 weight percent Al and 0.05 weight percent Fe
as the major impurities.

Preliminary calcinings to prepare large amounts of
$KAlO_2$ and low-temperature orthorhombic $KAlSiO_4$
were conducted using conventional resistance fur-
naces, either of the tube or box type. Temperatures
generally are known to ±20°C. Batches of 10–20 g
were calcined in 10 ml Pt crucibles with tight-fitting
lids. Compositions along the $KAlO_2$–SiO_2 join (Fig.
1) were prepared by weighing out the proper propor-
tions of potassium aluminate and quartz in 1-gram
quantities within the drybox. Mixtures were homoge-
nized under acetone, dried at 160°C, and homoge-
nized repeatedly while hot.

Quench experiments

Quench experiments were conducted in
80Pt/20Rh-wound furnaces controlled to within
±2°C by an a.c. Wheatstone bridge controller. Un-
less otherwise noted, samples were sealed in Pt cap-
sules and quenched in water. Typically, quantities of

from 10 to 100 mg were used. These were weighed after welding and after quenching. Capsules which leaked were easily identified by absorption of water during the quench. Temperature was monitored using a Pt/Pt10Rh thermocouple assembly calibrated *in situ* against the melting points of Au (1064°C) and Pd (1554°C). For some experiments, particularly those above 1500°C, temperature was monitored using an NBS-calibrated optical pyrometer. Uncertainty in temperature for quench experiments is estimated to be less than ±10°C, taking into consideration accuracy and precision of measurement devices, long-term instrumental drift, and thermal gradients.

To check on the possibility of potassium loss to the platinum capsules at elevated temperatures, energy-dispersive X-ray analysis was performed in conjunction with high-magnification SEM examination. It was found necessary to examine the capsules from runs in which melting occurred, to avoid interference from small particles adhering to the Pt. Analysis of a Pt capsule in which $(KAlO_2)_{40}(SiO_2)_{60}$ was melted at 1650°C showed no detectable K (estimated detection limit ≈ 0.2 wt%). The analysis was done at an accelerating potential of 20 kv.

Flux syntheses

Flux syntheses[1] of small single crystals (<2 mm) were performed using halide fluxes in an uncovered 5 ml platinum crucible heated inductively. Temperature was monitored with an optical pyrometer. Charges of 1–5 grams were stirred regularly with a Pt wire to promote chemical homogeneity during gradual melting. Fluorides vaporize as the temperature is increased to initiate reaction, but experiments were terminated while the halide content was such that an appreciable quantity of melt still existed. Samples were leached in water, dried with acetone, and sieved to provide suitable fractions for selection of single crystals or preparation of powder diffraction patterns.

X-ray diffraction

X-ray diffraction patterns were made from powders packed into a cavity of 0.07–0.15 mm depth cut into glass slides. A high-angle diffractometer calibrated with tungsten, silicon, and α-quartz was used. Nickel-filtered copper radiation was used with a scan speed of 0.25° 2θ per minute and a chart speed of 1° 2θ per inch.

---

[1] Refer to Duboin (1892) for a description of some early flux syntheses of potassium aluminosilicates.

Single crystals were investigated using an X-ray precession camera and Mo radiation, filtered and unfiltered. Precession photographs were used to determine symmetry and to aid in indexing powder patterns, from which cell parameters were calculated and refined by a least-squares computer program.

Energy-dispersive X-ray analysis

A scanning electron microscope and attached Si/Li detector were used to perform energy-dispersive X-ray analysis of K, Al, and Si in single crystals. Crystals were attached to a carbon substrate by evaporating a drop of 2 percent collodion solution in amyl acetate. The thickness of the resulting collodion film is estimated as less than 2000A. Calculation of the effect of this thickness on intensity ratios for K, Si, and Al $K\alpha$ radiation indicates that it should not interfere with semi-quantitative analysis when a normalization procedure is used (see Mulligan and Lapi, 1976). Before analysis, specimens were coated with 100–200A of carbon. Standards used were melted and quenched $(KAlO_2)_{40}(SiO_2)_{60}$, $(KAlO_2)_{50}(SiO_2)_{50}$, and $(KAlO_2)_{51}(SiO_2)_{49}$, from which smooth polished surfaces were prepared. Smooth uncontaminated portions of single-crystal faces were selected for analysis and oriented at the same angle relative to the beam and detector used for the standards. Aluminum and silicon intensities were determined using portions of the spectrum free of overlap. Use of low beam current (10^{-11} A) and moderate accelerating potential (20 kV), with the beam rapidly rastered over areas ~100 μm × 100 μm, minimized migration of potassium in the specimens due to heating.

Experimental results

$KAlSiO_4$

Quench experiments and solid-state synthesis. Results of quench experiments and solid-state synthesis of $KAlSiO_4$ compositions are summarized in Table 1 and Figure 2. To prepare a substantial quantity of $KAlSiO_4$ for quench experiments, $(KAlO_2)_{50}(SiO_2)_{50}$ was calcined at 950°C for a total of 135 hr with periodic grindings and homogenizations. Reaction, monitored by X-ray diffraction, was nearly complete after only a few hours. Traces of leucite and $KAlO_2$ solid solution were present, but disappeared with further equilibration. The product from these heat treatments yields a powder pattern similar in most respects to that reported by Smith and Tuttle (1957, Table 7) for orthorhombic $KAlSiO_4$. However our pattern (Table 3) does not contain the extra lines at
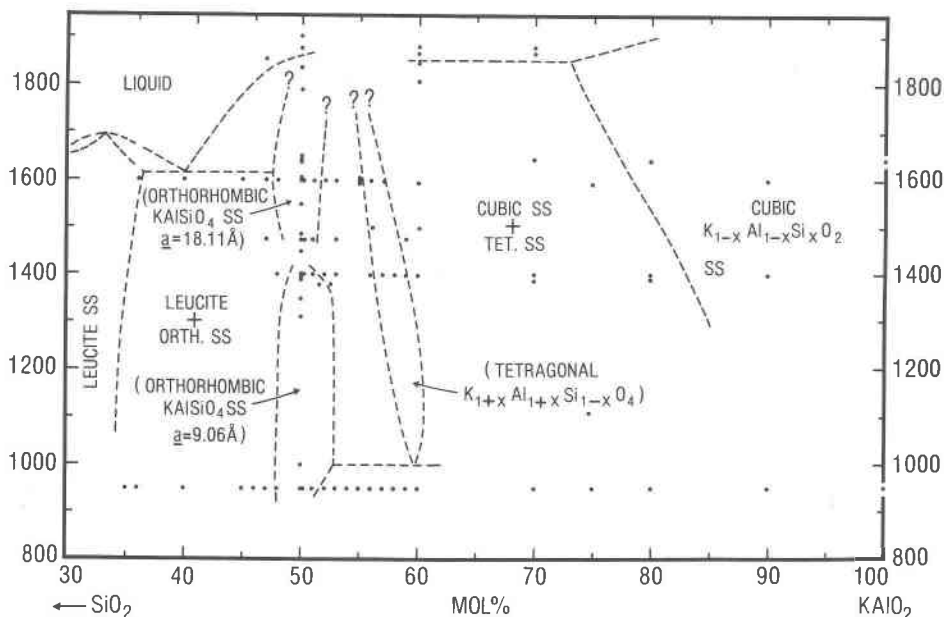
Fig. 2. *Synthesis* diagram for a part of the system $KAlO_2-SiO_2$ with tentative solid-solution limits. An *equilibrium* diagram will be published in a subsequent paper.

5.51, 4.484, 3.489, 3.267, and 2.901Å which are identified by Smith and Tuttle (1957, Table 7) as those of a second phase. Our material, when heated at 1400°C in a sealed Pt capsule, reveals no change other than a slight sharpening of lines, presumably from annealing. However, $KAlSiO_4$ synthesized at 1450–1485°C from $KAlO_2$ and SiO_2, as well as $KAlSiO_4$ synthesized at 950°C and then subjected to heating at 1640°C, yields a pattern (Table 4) essentially identical to that of Smith and Tuttle (1957) containing the extra lines. Single-crystal precession photographs (see below) show that the transition is from a low-temperature orthorhombic cell with $a = 9.057$, $b = 15.642$, $c = 8.582$Å to a higher-temperature orthorhombic cell with $a = 18.110$, $b = 15.600$, and $c = 8.560$Å. Details of the powder patterns for these two phases are given in Tables 3 and 4. Portions of the powder patterns showing the appearance of the extra lines are shown in Figure 3.

A single-phase orthorhombic material of composition $(KAlO_2)_{50}(SiO_2)_{50}$ showing the doubled unit cell is produced by heating at 1610°C followed by quenching. However, the form with the doubled cell has not been synthesized at temperatures below 1450° in any of the experiments thus far performed (Table 1, Fig. 2). Data in Table 1 demonstrate that if $KAlO_2$ is added to $KAlSiO_4$ with the doubled unit cell so that the final composition is

$(KAlO_2)_{52.5}(SiO_2)_{47.5}$, subsequent heating at 1380°C produces a nearly complete reversion to the form with the smaller unit cell. These facts lead us to conclude that the orthorhombic material with the smaller unit cell is indeed stable at the expense of the orthorhombic form with the doubled cell below $\sim$1450°C. The role of composition at the phase transition remains uncertain, and considerably more experimental work on closely-spaced compositions must be done before the phase diagram is determined.

Flux syntheses. Results of flux syntheses are summarized in Table 2. In contrast to the solid-state $KAlSiO_4$ synthesis at 950°C, flux synthesis at 1000°C using $(KAlO_2)_{50}(SiO_2)_{50}$ yielded hexagonal $KAlSiO_4$, with a powder pattern similar to that for synthetic kaliophilite reported by Smith and Tuttle (1957, Table 10). The hexagonal fluxed material, after heating at 1400°C in a sealed Pt capsule, has a powder pattern identical to that of orthorhombic $KAlSiO_4$ synthesized in the solid state of 950°C. When the fluxed material is heated at 1550 to 1600°C, the results again are essentially identical to those for the unfluxed material.

Precession photographs of flux-grown single crystals of orthorhombic $KAlSiO_4$ (Fig. 4) agree completely with the data reported by Kunze (1954) for orthorhombic $KAlSiO_4$ and satisfy $h00:h = 2n$ and

Table 1. Experimental data for the system $KAlO_2$–SiO_2

Left half

Composition $KAlO_2$ mole%	SiO_2	Initial Temp °C	Initial Time hr	Final Temp °C	Final Time hr	Results of X-ray Diffraction Analyses[b]
35	65	950	100			Lc
36	64	950[c]	96			
		1200[c]	16			
		1500[c]	64	1600[d]	4	Lc
45	55	950	48			
		1200[c]	64			
		1500[c]	16			Orth., extra lines+Lc
		1600[c]	4	1600[d]	24	Orth., extra lines+Lc
47	53	950	54			Lc+Orth., no extra lines
		1200[c]	64			
		1500[c]	16			Orth., extra lines+Lc
		1600[c]	2	1856[e]	0.15	Glass
47	53	950	54			Lc+Orth., no extra lines
				1473[d]	90	Orth., extra lines+Lc
47	53	950	54			Lc+Orth., no extra lines
		1600[c]	2	1500[d]	16	Lc+Orth., extra lines
48	52	950	108			
		1200[c]	64			
		1500[c]	16			Orth., extra lines
		1600[c]	2	1600[d]	20	Orth., extra lines
48	52	950	108			Orth., no extra lines +Lc+tr. Tet.
		1402[c]	88			Orth., no extra lines+Lc
		1404[c]	28			Orth., no extra lines+Lc
		1400[c]	38	1403[d]	28	Orth., no extra lines+Lc
50	50	950	135			Orth., no extra lines
				1395[d]	20	Orth., no extra lines
				1600[d]	7	Orth., extra lines
				1640[d]	15	Orth., extra lines+Tet.
		1400[c]	3			Orth., no extra lines
				1645[f]	10	Orth., extra lines
50	50	950[d]	135			Orth., no extra lines
		1605[d]	18			Orth., extra lines+Tet.
		1398[d]	27			Orth., extra lines+Tet.
		1396[d]	26			Orth., extra lines+Tet.
		1398[d]	219			Orth., extra lines+Tet.
		1350[c]	311			Orth., extra lines+Tet.
				1349[f]	50	Orth., extra lines of diminished intensity+Tet(?)
50	50	1475[c]	4			
		1485[c]	6			
		1450[c]	16	1450[c]	20	Orth., extra lines
50	50	1000[g] 0.5 1400[d]	47			Orth., no extra lines
		1400[d] 47 1650[d]	4			Orth., extra lines at 3.48, 3.26, 2.90
50	50	1310[g] 0.5 1550[c]	16			Orth., extra lines at 3.48, 2.90
50	50	950	135			
		1300[c]	2			
		1400[c]	2			
		1500[c]	16			
		1600[c]	6	1600[d]	24	Orth., extra lines
				1792[e]	0.01	Orth., extra lines
				1834[e]	0.08	Glass + Orth., extra lines
				1856[e]	0.15	Glass

Right half

Composition $KAlO_2$ mole%	SiO_2	Initial Temp °C	Initial Time hr	Final Temp °C	Final Time hr	Results of X-ray Diffraction Analyses[b]
50	50	950[d]	135			
		1404[d]	6			
		1405[d]	22			
		1404[d]	16			Orth., no extra lines
		1402[d]	32	1597[d]	18	Orth., extra lines
50.2	49.8	950[c]	54			Orth., no extra lines
		1200[c]	64			
		1500[c]	16	1600[d]	2	Orth., extra lines
50.2	49.8	950[d]	54			Orth., no extra lines
		1405[d]	4			Orth., no extra lines +Cubic ss
		1402[d]	17			Orth., no extra lines +Cubic ss
		1403[d]	12			Orth., no extra lines +tr. Tet.+tr. Cubic ss
		1403[d]	21			Orth., no extra lines +tr. Tet.
		1403[d]	21.5	1593[d]	17.5	Orth., no extra lines / Orth., extra lines
50.2	49.8	950	54			Orth., no extra lines
				1600[d]	2	Orth., extra lines
				1480[d]	168	Orth., extra lines
				1478[d]	19	Orth., no extra lines +tr. Orth., extra lines
51	49	950	96			Orth., no extra lines
				1600[d]	24	Orth., extra lines
				1473[d]	19	Orth., no extra lines +tr. Orth., extra lines
51	49	1401[d]	15			Orth., no extra lines +tr. Cubic ss
		1403[d]	19			Orth., no extra lines +tr. Tet.
		1405[d]	18	1595[d]	17	Orth., no extra lines / Orth., extra lines
51.5[h]	48.5[h]	1380[d]	11			Orth., extra lines of diminished intensity
52	48	950	55	1600	24	Orth., extra lines+Tet. / Orth., no extra lines +tr. Cubic ss
		1404[d]	9			Orth., no extra lines +Tet.+tr. Cubic ss
		1405[d]	7.5	1404	7.0	Orth., no extra lines +Tet.
52.5[i]	47.5[i]	1380[d]	131			Orth., very weak extra lines
53	47	950[c]	60			
		1200[c]	64			
		1500[c]	16			
		1600[c]	4	1600[d]	24	Orth., extra lines+Tet.
53	47	950[d]	60			
		1403[d]	5.5			Orth., no extra lines +tr. Cubic ss
		1404[d]	6			Orth., no extra lines +Tet.+Cubic ss
		1405[d]	10			Orth., no extra lines +Tet.+tr. Cubic ss
		1408[d]	23.5			Orth., no extra lines +Tet.+tr. Cubic ss
				1398[d]	50	Orth., no extra lines +Tet.

Table 1. Continued

Left half:

Composition KAlO₂ SiO₂ mole%		Heat Treatment Initial Temp °C / Time hr	Final Temp °C / Time hr	Results of X-ray Diffraction Analyses[b]
55	45	1600[c] 5; 1600[c] 7	1600[d] 10	Tet.+Orth. (tr.)
55	45	1605[d] 41		Tet.+Cubic ss+Orth. (with extra lines?)
		1595[d] 17		Tet.+Cubic ss+tr. Orth. (extra lines?)
			1595[d] 33	Tet.
56	44	950 96; 1404[d] 3		Orth., no extra lines +tr. Cubic ss
		1405[d] 20.5		Orth., no extra lines +Tet.+Cubic ss
		1404[d] 67		Orth., no extra lines +Tet.+Cubic ss
		1404[d] 8		Tet.+Orth.+tr. Cubic ss
		1404[d] 15	1405[d] 14	Tet.+tr. Orth. / Tet.+tr. Orth.
56	44	950 96; 1200[c] 64; 1500[c] 16; 1600[c] 4	1600[d] 24	Tet.
57	43	950 50; 1200[c] 16; 1500[c] 64; 1600[c] 4	1600[d] 24	Tet.+tr. Cubic
57	43	950 50; 1404[d] 10		Orth., no extra lines +Tet.+Cubic ss
		1404[d] 45	1403[d] 23.5	Tet.+tr. Orth.+tr. Cubic ss / Tet.
58	42	950 50; 1402[d] 46		Orth., no extra lines +Tet.+Cubic ss
		1403[d] 14.5		Tet.+Orth., no extra lines+Cubic ss
		1403[d] 17.5		Tet.+tr. Orth.+Cubic ss
		1403[d] 19.5	1403[d] 20.5	Tet.+tr. Orth.+tr Cubic ss / Tet.

Right half:

Composition KAlO₂ SiO₂ mole%		Heat Treatment Initial Temp °C / Time hr	Final Temp °C / Time hr	Results of X-ray Diffraction Analyses[b]
59	41	950 96; 1404[d] 14		Tet.+Orth., no extra lines+Cubic ss
		1402[d] 18.5		Tet.+Orth.+Cubic ss
		1402[d] 12	1403[d] 191.5	Tet.+tr. Cubic ss / Tet.+tr. Cubic ss
59	41	950 96	1480[d] 168	Tet.+Cubic ss
60	40	1595[d] 8	1592[c] 10	Tet.+Cubic ss (tr.)
70	30	1400[c] 18		Cubic ss+Tet. (tr.)+Orth.
		1392[c] 12		Cubic ss+Tet.+Orth. (tr.)
		1402[c] 19		Cubic ss+Tet.
		1400[d] 111	1645[d] 6	Cubic ss+Tet.
75	25	1595[c] 12		Cubic ss+Tet. (tr.)
80	20	1400[c] 21		Cubic ss+Orth.+Tet. (tr.)
		1400[c] 9		Cubic ss+Tet.+Orth. (tr.)
		1400[c] 11		Cubic ss+Tet.+Orth. (tr.)
		1395[c] 3		Cubic ss+Tet.+Orth. (tr.)
		1400[d] 91	1395[d] 50; 1640[d] 24	Cubic ss+Tet. (tr.) / Cubic ss+Tet. (tr). / Cubic ss
90	10	1400[c] 12		ps. cubic ss
		1398[c] 5		ps. cubic ss
		1400[c] 13		ps. cubic ss
		1400[c] 7	1399[d] 12	Cubic (?) ss / ps. cubic
100	0	1645[d] 1.0		

[a] Successive heat treatments in this column indicate that the specimen had all the preceding initial heat treatments within its group

[b] tr. – trace; Orth., no extra lines – orthorhombic KAlSiO₄; Orth., extra lines – orthorhombic phase with doubled a, extra lines at 5.49, 4.17, 3.48, and 2.90A; Tet. – tetragonal $K_{1+x}Al_{1+x}Si_{1-x}O_4$; Cubic – cubic $K_{1-x}Al_{1-x}Si_xO_2$; ps. cubic – pseudocubic KAlO₂; ss – solid solution; Lc – KAlSi₂O₆

[c] Experiment removed from furnace and cooled in air

[d] Sealed experiment quenched in water

[e] Experiment performed in inductively heated Pt60/Rh40 capsules; air cooled

[f] Unsealed capsule, cooled in air

[g] From KF flux synthesis

[h] Specimen made by adding KAlO₂ to previously equilibrated KAlSiO₄ after final heat treatment at 1349°C for 50 hrs

[i] Prepared by adding more KAlO₂ to previous specimen of 51.5:48.5

Table 2. Flux synthesis of single crystals for X-ray diffraction

Al/Si Atomic Ratio	Charge[a]	Flux	Charge/Flux Weight Ratio	Temp.[b] °C	Time hr	Major Crystalline Phases After Treatment[c]
3:2	Al_2O_3+SiO_2	KF	1:19	1300	0.75	−150 mesh fraction: Tet. + Orth. + Cubic
3:2	K_3AlF_6+SiO_2	KF	1:5.67	1250	4.0	−150 mesh fraction: Orth. + Tet.
3:1	Al_2O_3+SiO_2	KF	1:19	1300	0.9	−150 mesh fraction: Tet. + Cubic
3:1	Al_2O_3+SiO_2	KF	1:4	1000	0.33	Orth. + Cubic + unidentified phase with strong 2.99A peak
2:1	$KAlO_2$+SiO_2	KF	1:3.33	1000	0.75	Cubic + Orth. + Tet.
1:1	$KAlO_2$ +SiO_2	KF	1:15	1000	0.5	Hex.
1:1	Al_2O_3+SiO_2	$KCl_{.5}F_{.5}$	1:19	950	1.0	Orth. + $KAlSi_2O_6$
1:1	Al_2O_3+SiO_2	KF	1:9	1310	0.5	Orth. + Tet.
1:1	Al_2O_3+SiO_2	KF	1:4	1000	0.75	Orth. + Tet.
1:1	K_3AlF_6+SiO_2	KF	1:9	1250	3.0	−48 + 115 mesh fraction: Orth. + Tet.
1:1	Al_2O_3+SiO_2	KF	1:19	1300	0.75	−48 + 115 mesh fraction: Orth.
1:1	Al_2O_3+SiO_2	KNO_3	unknown, large excess KNO_3	500	15.5	α-quartz + α-alumina

[a] Molar ratio of charge constituents was adjusted to yield the desired Al/Si atomic ratio.

[b] The indicated temperatures can only be considered approximations because of the great departure from blackbody conditions. No attempt should be made to compare these temperatures with those reported for quench experiments.

[c] In all cases, excess KF and other water solubles were removed by leaching 16 hours or more in hot water. Thus, phases observed should not be interpreted as being an equilibrium phase assemblage.

Hex. – hexagonal $KAlSiO_4$, pattern identical to synthetic kaliophilite of Smith and Tuttle (1957).
Orth. – orthorhombic $KAlSiO_4$ with no extra lines
Tet. – tetragonal $K_{1+x}Al_{1+x}Si_{1-x}O_4$
Cubic – cubic $K_{1-x}Al_{1-x}Si_xO_2$

$00l: l = 2n$. Also, $h0l: h + l = 2n$ is nearly satisfied but for weak (201) and (205) reflections. The space group then appears to be $P2_12_12$. It is noteworthy that this lower-temperature orthorhombic form is dimensionally hexagonal, whereas the higher-temperature orthorhombic form (see below) is not.

Precession photographs showing the effects of heating flux-grown orthorhombic $KAlSiO_4$ to 1650°C are presented in Figure 4. The heated crystals appear to have the same diffraction pattern for $[0kl]$ and $[h0l]$ as the lower-temperature form. Most important is the fact that the $[hk0]$ and $[hk1]$ photographs show doubling of the a axis. The new orthorhombic cell has diffraction symmetry $P*a*$, indicating $P2_1am$, $Pma2$, or $Pmam$.

An energy-dispersive X-ray analysis of a single crystal of orthorhombic material synthesized in flux at 1250°C and heated at 1610°C for 10 hr showed it to be, on a mole percent basis, $(K_2O)_{24.5\pm1}$ $(Al_2O_3)_{24.5\pm1}(SiO_2)_{51\pm2}$. The analysis should be regarded as semi-quantitative; it does not include fluorine, and the assumption was made that K, Al, and Si

are present as oxides. This crystal gave precession photographs similar to the ones in Figure 4 c, d except for differences attributable to twinning about c.

Tetragonal $K_{1+x}Al_{1+x}Si_{1-x}O_4$

Quench experiments and solid state synthesis. X-ray powder diffraction patterns of $(KAlO_2)_{70}(SiO_2)_{30}$ heated at $\sim 1400°C$ initially showed principal lines of orthorhombic $KAlSiO_4$ and of $K_{1-x}Al_{1-x}Si_xO_2$ solid solution. Continued heating in sealed Pt capsules with intermediate grindings resulted in an increase in intensity of a line at 3.17A with concomitant decrease in intensity of the principal $KAlSiO_4$ line at 3.11A.

Existence of a phase between $K_{1-x}Al_{1-x}Si_xO_2$ and $KAlSiO_4$ on the tectosilicate join is necessary to explain this (Fig. 2). Material synthesized from $(KAlO_2)_{55}(SiO_2)_{45}$ at 1600°C with intermediate crush-

Table 3. X-ray powder diffraction data for low-temperature orthorhombic $KAlSiO_4$[a/]

d_{obs}	hkl[b/]	$2\theta_{obs}$[c/]	$2\theta_{calc}$[c/]	I_{obs}
6.23	101	14.20	14.21	4
5.79	021	15.29	15.32	4
4.521	200/130	19.62	19.59/19.63	4
4.286	002	20.71	20.68	11
3.996	131	22.23	22.22	1
3.877	211	22.92	22.90	7
3.563	221/041	24.97	24.96/25.00	24
3.477	122	25.60	25.62	1
3.422	230	26.02	26.04	18
3.312	141	26.90	26.90	7
3.175	231	28.08	28.07	5
3.112	202/132	28.66	28.64/28.67	100
2.959	310/240/150	30.18	30.13/30.17/30.20	3
2.816	320	31.75	31.75	2
2.798	311/241/151	31.96	31.92/31.96/31.99	23
2.688	023	33.30	33.32	6
2.674	232	33.48	33.49	8
2.612	330/060	34.31	34.30/34.37	31
2.577	123/250	34.79	34.80/34.83	2
2.504	160	35.83	35.82	1
2.4934	061	35.99	35.98	1
2.4353	242/152	36.88	36.86/36.89	1
2.4138	133	37.21	37.17	1
2.3890	340/213	37.62	37.60/37.61	1
2.3553	322	38.18	38.19	1
2.2631	400	39.80	39.78	2
2.2582	260	39.89	39.87	1
2.2372	143	40.28	40.28	3
2.2308	070/332/062	40.40	40.33/40.39/40.45	9
2.1868	261	41.25	41.29	1
2.1628	162	41.73	41.72	2
2.1446	004	42.10	42.08	8
2.1088	421	42.85	42.86	3
2.1041	171	42.95	42.97	3
2.0760	430/303	43.56	43.54/43.55	5

a/ Synthesized by heating at 950°C for 135 hr, with intermediate grindings.

b/ Indexed on the basis of an orthorhombic primitive unit cell. Least-squares refined dimensions: $\underline{a}$=9.057(2)A, $\underline{b}$=15.642(2)A, $\underline{c}$=8.582(2)A, volume = 1215.$\overline{7}$(3)A.

c/ CuKα_1 radiation, λ = 1.540598A.

Table 4. X-ray powder diffraction data for the high-temperature orthorhombic phase[a/]

d_{obs}	hkl[b/]	$2\theta_{calc}$[c/]	$2\theta_{obs}$[c/]	I_{obs}
6.21	201	14.23	14.25	2
5.78	021	15.36	15.33	6
5.49[d/]	121	16.12	16.13	2
4.699	311	18.85	18.87	2
4.532	400	19.59	19.57	4
4.505	230	19.67	19.69	6
4.277[d/]	002	20.74	20.75	11
4.168[d/]	321	21.29	21.30	1
3.992	231	22.27	22.25	2
3.938	330	22.55	22.56	2
3.875	411	22.92	22.93	3
3.580	331	24.86	24.85	2
3.558	421	24.99	25.01	13
3.551[d/]	041	25.07	25.06	12
3.482[d/]	141	25.56	25.56	10
3.413	430	26.08	26.09	3
3.302[d/]	241	26.96	26.98	2
3.259[d/]	511	27.32	27.34	6
3.249	132	27.41	27.43	2
3.169	431	28.11	28.14	14[e/]
3.107	402/232	28.68/28.73	28.71	100
2.971	530	30.04	30.05	6
2.951[d/]	250	30.28	30.26	3
2.900[d/]	332	30.82	30.81	3
2.816	620	31.76	31.75	2
2.800	611	31.93	31.94	13
2.790	251	32.07	32.05	15
2.722	203	32.89	32.88	1
2.679	023	33.41	33.42	4
2.670	432	33.55	33.54	3
2.611	630	34.33	34.32	24
2.600	060	34.47	34.47	21
2.575	160	34.83	34.82	3
2.547	313	35.24	35.21	1
2.4961	631	35.94	35.95	1
2.4461	711	36.72	36.71	2
2.4100	233	37.26	37.28	2
2.3179	730	38.85	38.82	3
2.3122	333	38.94	38.92	3
2.2636	800	39.79	39.79	2
2.2533	460	39.96	39.98	2
2.2287	070	40.44	40.44	12
2.2068	162	40.88	40.86	2
2.1792	461	41.38	41.40	1
2.1568	071	41.87	41.85	2
2.1504	343	41.96	41.98	3
2.1402	004	42.20	42.19	10
2.1074	821	42.89	42.88	2

a/ Synthesized at 950°C, 135 hr with intermediate grindings, sealed in Pt capsule, heated at 1600±20°C, 7 hr, quenched in water.

b/ Indexed on the basis of an orthorhombic primitive unit cell. Least-squares refined dimensions: $\underline{a}$=18.110(3)A, $\underline{b}$=15.600(3)A, $\underline{c}$=8.560(2)A, volume = 2418.$\overline{2}$(5)A^3.

c/ CuKα_1 radiation, λ = 1.540598A.

d/ Lines also observed by Smith and Tuttle (1957) and attributed by them to a possible second phase.

e/ Abnormally large intensity indicates small amount of tetragonal $K_{1+x}Al_{1+x}Si_{1-x}O_4$.

ings and grindings produced a pattern containing no trace of $KAlO_2$ solid solution and with only a trace of $KAlSiO_4$. The powder diffraction pattern can be completely indexed on the basis of the tetragonal unit

cell ($a = 8.943$, $c = 5.221A$) determined from the precession photographs. It was thought at first that this pattern might represent a disordered hexagonal phase structurally related to tridymite. Indeed, the pattern could be partially indexed on the basis of a hexagonal cell with $a = 10.44$, $c = 8.94A$; however, several peaks of low intensity deviated from the calculated values by as much as $0.25°$ 2θ. Precession photographs of flux-synthesized crystals proved unequivocally that the actual symmetry is tetragonal. A tabulation of calculated $vs.$ observed d-spacings for the tetragonal phase is given in Table 5.

Flux synthesis. $(Al_2O_3)_{43}(SiO_2)_{57}$ heated to

a.   **b.**

c.   **d.**

Fig. 4. Precession photographs of orthorhombic $KAlSiO_4$ synthesized from K_3AlF_6 and SiO_2 in KF flux at 1250°C (a,b) and subsequently heated in sealed Pt capsule at 1610°C for 10 hr (c,d). Zr-filtered Mo radiation was used except for b and c (unfiltered). a, c—[hk0]; b, d—[hk1].

a)

Fig. 3. Portions of powder patterns of orthorhombic $KAlSiO_4$. (a) Synthesized at 950°C, 135 hr. This pattern is typical of single-phase $KAlSiO_4$ heated for extended periods at temperatures up to 1400°C. (b) Synthesized at 1605°C, 18 hr, annealed at ~1400°C, 53 hr. This pattern is typical of single-phase $KAlSiO_4$ heated for extended periods above 1600°C, and shows development of extra lines discussed in text.

~1300°C with excess KF yielded crystals of the tetragonal phase plus some cubic $K_{1-x}Al_{1-x}Si_xO_2$ (Table 2). Precession photographs of single crystals (Fig. 5) clearly indicate a body-centered tetragonal symmetry ($h + k + l = 2n$) with Laue group $4/mmm$. As there are no other special extinctions, five space groups including $I4/mmm$ are possibilities. The relation between cell dimensions of the tetragonal phase and the orthorhombic $KAlSiO_4$ is as follows: tetragonal c is equivalent to one-third orthorhombic b, and tetragonal a is approximately equal to the average of orthorhombic a and c.

An energy-dispersive X-ray analysis of the single crystal used for precession work showed it to be, on a mole percent basis, $(K_2O)_{27.5\pm1}(Al_2O_3)_{27.5\pm1}(SiO_2)_{45\pm2}$. The analysis should be regarded as semi-quantitative; fluorine could not be determined and in computing this analysis it was assumed that K, Al, and Si are present as oxides.

$K_{1-x}Al_{1-x}Si_xO_2$ solid solutions

Quench experiments and solid-state syntheses. Preliminary experiments (Table 1) have indicated a considerable solubility of SiO_2 in cubic $KAlO_2$ at temperatures of 1400 to 1600°C. Limits of solid solution have not yet been established precisely, but lie between 20 and 25 mole percent SiO_2 at 1600°C. The addition of SiO_2 apparently lowers the phase transition temperature in this material or alters the kinetics enough to allow quenching the cubic form to room temperature. The least-squares refined cell parameter for the SiO_2-rich end member synthesized at 1645°C is $a = 7.644$A. A tabulation of observed vs. calculated d-spacings is given in Table 6.

Flux syntheses. Flux syntheses with two different types of starting materials (Table 2) yielded cubic solid solutions. Although $KAlO_2$ reacts with atmospheric moisture even at room temperature to "melt" in its own liquid of hydration, the solid-solution end member apparently is insoluble in hot water and can easily be separated from KF by water-leaching. Precession photographs and powder diffraction data (Table 6) indicate that this solid solution is face-centered cubic with hkl: h, k, l all odd or all even, and that it belongs to the Laue group $m3m$.

Conclusions

Additional lines occurring at 5.49, 4.168, 3.482, 3.259, and 2.900A in powder patterns of orthorhombic $KAlSiO_4$ heated at 1600–1650°C can be completely accounted for by a doubling of the a dimension of the unit cell described by Kunze (1959). The doubling of the a axis is proved by single-crystal precession photographs of flux-grown material. The experimental evidence disproves the interpretation of the extra lines as a second phase as postulated by

Table 5. X-ray powder diffraction data for tetragonal $K_{1+x}Al_{1+x}Si_{1-x}O_4$[a]

d_{obs}	hkl[b]	$2\theta_{obs}$[c]	$2\theta_{calc}$[c]	I_{obs}
6.32	110	14.01	13.99	11
4.510	101	19.67	19.67	28
4.471	200	19.84	19.84	10
3.168	211/220	28.15	28.08/28.20	100
2.827	310	31.62	31.61	25
2.612	002	34.31	34.32	28
2.588	301	34.63	34.62	58
2.4150	112	37.20	37.23	16
2.2544	202	39.96	39.96	4
2.2415	321	40.20	40.22	22
2.2372	400	40.28	40.31	33
2.1083	330	42.86	42.87	6
2.0015	411/420	45.27	45.24/45.32	6
1.7534	510	52.12	52.11	3
1.7076	103	53.63	53.60	3
1.6973	402	53.98	53.95	2
1.6909	431	54.20	54.16	6
1.6405	332	56.01	56.03	7
1.5959	213	57.72	57.72	7
1.5876	422	58.05	58.06	5
1.5821	521/440	58.27	58.26/58.32	8
1.5332	530	60.32	60.30	5
1.5028	303	61.67	61.66	11
1.4902	600	62.25	62.24	6
1.4557	512	63.90	63.89	5
1.4251	323	65.44	65.46	1
1.3053	004	72.33	72.33	1
1.2944	602	73.04	73.04	4
1.2918	631	73.21	73.22	8

[a] Synthesized from $(KAlO_2)_{.55}(SiO_2)_{.45}$ by three heat treatments at 1600±20°C followed by quenching in water and grinding (22 hr total heating); product was nearly-single-phase, with trace of $KAlSiO_4$.

[b] Indexed on the basis of a tetragonal body-centered unit cell. Least-squares refined dimensions: a=8.943(1)A, c=5.221(1)A, volume = 417.54(8)A^3.

[c] CuKα_1 radiation, λ = 1.540598A.

Smith and Tuttle (1957). Our data support reversibility of the change from orthorhombic $KAlSiO_4$ ($a = 9.057$, $b = 15.642$, $c = 8.582$A) to the higher-temperature orthorhombic $KAlSiO_4$ with the larger
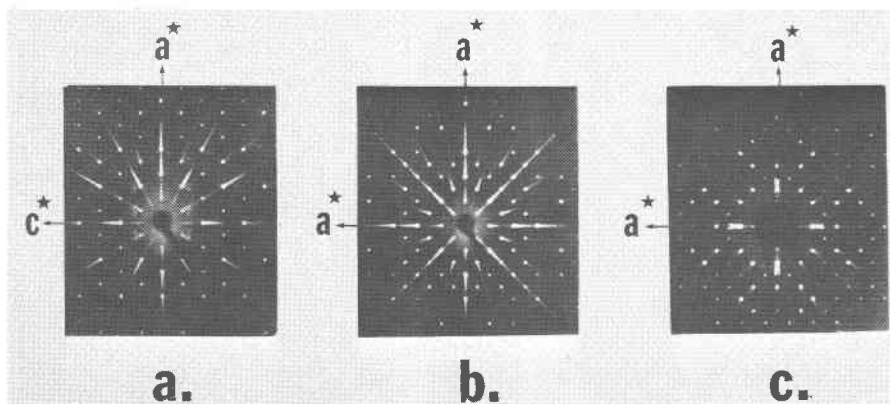

Fig. 5. Precession photographs of tetragonal $K_{1+x}Al_{1+x}Si_{1-x}O_4$ synthesized from $(Al_2O_3)_{43}(SiO_2)_{57}$ in KF flux at 1300°C (refer to Table 2). Zr-filtered Mo radiation was used. a—[h0l], b—[hk0], c—[hk1].

Table 6. X-ray powder diffraction data for cubic $K_{1-x}Al_{1-x}Si_xO_2$[a]

d_{obs}	$hk\ell$[b]	$2\theta_{obs}$[c]	$2\theta_{calc}$[c]	I_{obs}
4.414	111	20.10	20.10	18
2.701	220	33.13	33.12	100
2.3059	311	39.03	39.05	5
2.2068	222	40.86	40.86	7
1.9115	400	47.53	47.54	3
1.7541	331	52.10	52.11	2
1.5600	422	59.18	59.16	18
1.3514	440	69.50	69.50	5
1.2923	531	73.18	73.19	2
1.2086	620	79.19	79.18	3

[a] Heat treatment of $(KAlO_2)_{.70}(SiO_2)_{.30}$ at 1392 to 1400°C (160 hours total) followed by heating at 1645±10°C (6 hours); product contains trace tetragonal phase.

[b] Indexed on the basis of a cubic face-centered unit cell. Least-squares refined dimensions: $\underline{a}$=7.644(1)A, volume = 446.72(9)A^3.

[c] $CuK\alpha_1$ radiation; λ = 1.540598A.

cell (a = 18.110, b = 15.600, c = 8.560A) in the range 1380–1485°C, at least in the presence of excess $KAlO_2$. The tetragonal phase $K_{1+x}Al_{1+x}Si_{1-x}O_4$ is stable at the expense of cubic $K_{1-x}Al_{1-x}Si_xO_2$ and orthorhombic $KAlSiO_4$ over a temperature range extending at least from 1400 to 1600°C. No evidence has been found for the existence of a specific compound with composition $K_2Al_2SiO_6$ at 1400–1600°C. Rather, the maximum solubility of SiO_2 in cubic $KAlO_2$ suggests $K_3Al_3SiO_8$ as a limiting composition of this series, which corresponds to $K_{1-x}Al_{1-x}Si_xO_2$ with x = 0.25. The cubic nature of this phase suggests that it is the one observed by Bowen (1917), Weyberg (1908), and others. The exact range of solid solution as a function of temperature and the effect of composition on the cubic/non-cubic phase transition must await further experimentation now underway in our laboratory. Subsolidus reactions along the join $KAlSiO_4$–$KAlO_2$ are very sluggish, and repeated grinding appears necessary for equilibration even at temperatures approaching 1600°C. Short-term experiments may sometimes be expected to produce metastable results, as shown by the data in Tables 1 and 2.

References

Arakelyan, O. T. (1960) Polymorphism and isomorphism of some phases of the system Na_2O (or K_2O)–Al_2O_3–Fe_2O_3. Khim. i Prakt. Primen. Silik., Inst. Khim Silik., Akad. Nauk SSSR, p. 63–71.

Barth, T. F. W. (1935) Non-silicates with cristobalite-like structures. J. Chem. Phys., 3, 323–325.

Bowen, N. L. (1917) The sodium–potassium nephelites. Am. J. Sci., 43, 115–132.

Brownmiller, L. T. (1935) A study of the system lime–potash–alumina. Am. J. Sci., 29, 260–275.

Duboin, A. (1892) Reproduction de la leucite, de la cryolithe potassique et de la nepheline potassique. Bull Soc. fr. Mineral., 15, 191–195.

Hosler, W. R., T. Negas and S. W. Petty (1976) Analysis of AVCO Mark VI C Channel electrodes after long duration test. Proc. 15th Symp. Engineering Aspects of Magnetohydrodynamics, Philadelphia, May 24–26, 1976. (late paper).

Karr, C., Jr., P. Waldstein and J. J. Kovach (1974) Composition of fly ash from a coal fired MHD [magnetohydrodynamic] generator with potash seed. J. Inst. Fuel, 47, 177–180.

Kunze, G. (1954) Uber die rhombische Modifikation von $KAlSiO_4$ in Anlehrung an den Kalsilit. Beitr. Mineral. Petrogr., 4, 99–129.

Li, C., A. F. Reid, and S. Saunders (1971) Nonstoichiometric alkali ferrites and aluminates in the systems $NaFeO_2$–TiO_2, $KFeO_2$–TiO_2, $KAlO_2$–TiO_2, and $KAlO_2$–SiO_2. J. Sol. State Chem., 3, 614–620.

Mulligan, T. J., and L. A. Lapi (1976) Normalization procedure for X-ray microanalysis which accounts for fluctuations in beam current. In O. Johari, Ed., Scanning Electron Microscopy/1976, p. 195–198. Chicago, IIT Research Institute.

Otsubo, Y., K. Yamaguchi and Y. Kawamura (1962) Thermal behavior of alkali metal aluminates. Nippon Kagaku Zasshi, 83, 352–353.

Perrota, A. J., and J. V. Smith (1965) The crystal structure of kalsilite, $KAlSiO_4$. Mineral. Mag., 35, 588–595.

Plante, E. R., C. D. Olson and T. Negas (1975) Interaction of K_2O with slag in open cycle coal fired MHD. Sixth Int. Conf. on Magnetohydrodyn. Electr. Power Generation, 2, 211–218.

Rigby, G. R. and H. M. Richardson (1947) The occurrence of artifical kalsilite and allied potassium aluminum silicates in blast-furnace lining. Mineral. Mag., 28, 75–88.

Sahama, Th. G. and J. V. Smith (1957) Tri-kalsilite, a new mineral. Am. Mineral., 42, 286.

Schairer, J. F. and N. L. Bowen (1955) The system K_2O–Al_2O_3–SiO_2. Am. J. Sci., 253, 681–746.

Smith, J. V. and O. F. Tuttle (1957) The nepheline–kalsilite system. I. X-ray data for the crystalline phases. Am. J. Sci., 255, 282–305.

Weyberg, Z. (1908) Uber das Aluminosilikat $K_2Al_2SiO_6$. Centralbl. Mineral. Geol. Paleont., 11, 326–330.

Yamaguchi, A. (1970) $K_2O \cdot Al_2O_3 \cdot SiO_2$ and $K_2O \cdot Al_2O_3$. Yogyo Kyoki Shi, 78, 74–75.